

# Fine-grained Domain Adaptive Crowd Counting via Point-derived Segmentation

Yongtuo Liu, Dan Xu, Sucheng Ren, Hanjie Wu, Hongmin Cai, *Member, IEEE*,  
and Shengfeng He, *Senior Member, IEEE*

**Abstract**—Despite the remarkable progress in supervised crowd counting, a large performance drop is usually observed when deploying the trained model in the wild. This is mainly caused by the domain shift between the training and deployment crowd scenes. Existing domain adaptation methods for crowd counting view each crowd image as a whole and reduce domain discrepancies on crowds and backgrounds simultaneously. However, we argue that these methods are suboptimal, as crowds and backgrounds have quite different characteristics and backgrounds may vary dramatically in different crowd scenes (see Fig. 1). This makes crowds not well aligned across domains together with backgrounds in a holistic manner. To this end, we propose to untangle crowds and backgrounds from crowd images and design fine-grained domain adaption methods for crowd counting. Different from other tasks which possess region-based fine-grained annotations (e.g., segments or bounding boxes), crowd counting only annotates one point on each human head, which impedes the implementation of fine-grained adaptation methods. To tackle this issue, we propose a novel and effective schema to learn crowd segmentation from point-level crowd counting annotations in the context of Multiple Instance Learning. We further leverage the derived segments to propose a crowd-aware fine-grained domain adaptation framework for crowd counting, which consists of two novel adaptation modules, i.e., Crowd Region Transfer (CRT) and Crowd Density Alignment (CDA). Specifically, the CRT module is designed to guide crowd features transfer across domains beyond background distractions, and the CDA module dedicates to constraining the target-domain crowd density distributions. Extensive experiments on multiple cross-domain settings (i.e., Synthetic  $\rightarrow$  Real, Fixed  $\rightarrow$  Fickle, Normal  $\rightarrow$  BadWeather) demonstrate the superiority of the proposed method compared with state-of-the-art methods.

## I. INTRODUCTION

Over the past few years, crowd counting has drawn increasing attention in the field of computer vision due to its fundamental role in social management [17], [31], [45], such as traffic monitoring, crowd congestion warning, etc. Recently, remarkable progress has been achieved for supervised crowd counting [65], [87], [90]. However, due to the phenomenon known as domain shift or dataset bias [70], performance degrades a lot when trained models are deployed in some unseen crowd scenes, which limits the massive real-world applications. To fill the performance gap, the direct solution

Yongtuo Liu, Sucheng Ren, Hanjie Wu, Hongmin Cai, and Shengfeng He are with the School of Computer Science and Engineering, South China University of Technology, Guangzhou, China. E-mail: cs-manlyt@mail.scut.edu.cn, oliverrensu@gmail.com, cshanjiwewu@gmail.com, {hmcai, hesfe}@scut.edu.cn.

Dan Xu is with the Department of Computer Science and Engineering, Hong Kong University of Science and Technology. E-mail: danxu@cse.ust.hk.

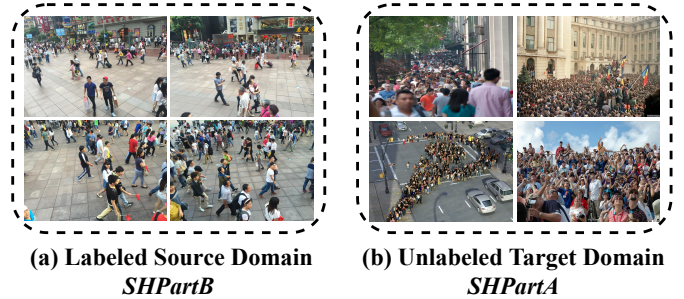


Fig. 1: Crowd images from *SHPartB* (a) and *SHPartA* (b) datasets [90], respectively. As can be seen, backgrounds vary dramatically across crowd domains or even in each domain. For instance, the backgrounds in *SHPartB* are mainly grounds whereas various backgrounds appear in *SHPartA* including buildings, trees, sky, *etc.*

is to label abundant images in the target crowd scene. Nevertheless, the labeling is really onerous as it requires labeling each individual in crowd images.

To tackle this issue, one promising way is to introduce Unsupervised Domain Adaptation (UDA) to transfer essential knowledge learned from a labeled source domain to the related but unlabeled target domain [53]. Recently, some methods propose to apply UDA for cross-domain crowd counting, including pixel-level adaptation methods [76] and feature-level adaptation methods [19]–[21]. The pixel-level methods employ unpaired style transfer [94] to translate source-domain crowd images to the target-domain ones, and then train the target-domain crowd counter in a supervised manner. Nevertheless, it remains a challenge to ensure the quality of the generated images, especially in crowd scenes which typically show extreme visual conditions [76]. Alternatively, the feature-level methods reside in generating domain-invariant feature representations by reducing statistical distances [21] or utilizing adversarial training [19], [20]. Compared to pixel-level methods, such methods can achieve competitive performance and work more conveniently, thus dominating the existing literature.

Despite the promising results, all existing domain adaption methods for crowd counting [19]–[21], [76] regard each crowd image as a whole and reduce domain discrepancies on crowds and backgrounds simultaneously. However, crowds and backgrounds have quite different characteristics, and backgrounds may vary dramatically in different crowd scenes (see Fig. 1), which makes crowds not well aligned across domains together with the backgrounds in a holistic manner.

To this end, we propose to untangle crowds and backgrounds from crowd images and design fine-grained domain adaption methods for crowd counting. One main challenge here is that different from other computer vision tasks which possess region-based annotations (e.g., segments or bounding boxes), crowd counting only annotates one point on each human head, which impedes the implementation of fine-grained adaptation methods. To solve this problem, we propose to learn crowd segmentation from the available crowd counting annotations (namely Point-derived Crowd Segmentation) without extra labeling efforts. Specifically, we derive region-based segmentation from the point-level annotations by learning label statistics in the context of Multiple Instance Learning [49]. The rationale behind this design is that although crowd counting annotations does not specify crowd segmentation, the annotated head points still entail the information on where crowds appear and how crowds look like from a statistical perspective. We further leverage the derived segments to propose a Crowd-aware fine-grained domain Adaptation framework for Crowd Counting (CACC), which consists of two novel adaptation modules, namely Crowd Region Transfer (CRT) and Crowd Density Alignment (CDA). The two modules are designed for two different adaptation purposes, i.e., feature transfer and density alignment. First, to guide crowd features transfer across domains beyond background distractions, we introduce the CRT module to incorporate the derived segments into multi-level domain classifiers to extract domain-invariant crowd features. Second, to align target-domain crowd density distributions, we design the CDA module to generate segmentation-guided probabilistic pseudo labels to dynamically constrain the density maps generation.

In summary, the contributions are organized as follows:

- We propose to learn crowd segmentation from point-level crowd counting annotations in the context of Multiple Instance Learning [49] to disentangle crowds from backgrounds for better adaptation across domains.
- We propose a crowd-aware fine-grained domain adaption framework for crowd counting, which exploits the point-derived segments to guide crowd features transfer and crowd density alignment beyond background distractions. To the best of our knowledge, our work is the first attempt to explore fine-grained domain adaptation methods for crowd counting.
- Our method outperforms previous best approaches by a large margin in the widely-used Synthetic-to-Real adaptation scenario.

## II. RELATED WORK

### A. Crowd Counting

Early works for crowd counting are mainly based on hand-crafted features (e.g., SIFT, Fourier Analysis, HOG) to estimate crowd counts by either regression [8], [22], [30] or object detection [34], [75], [79]. In these years, various CNN-based methods have advanced the performance of crowd counting. Most of them are dedicated to handle various challenges of crowd counting in an supervised manner, e.g., large scale variations [4], [23], [24], [32], [36], [37], [46], [61], [90],

hand-crafted gaussian kernels [35], [48], [74], uncertainty [51], [54], enhancing crowd features [42], [50], [67], [85], [86], extra constraints [33], [63], [81], *etc.* Besides the supervised methods, several approaches focus on relieving the labeling burdensome. They can be broadly categorized into semi-supervised methods [5], [40], [55], [68], [91], [93], weakly-supervised methods [83], self-supervised methods [38], [39] and unsupervised methods [14], [60].

These generic crowd counters can achieve promising performance in public datasets, whereas they do not focus on solving the domain shift problem, which hurts their generalization performance in real-world application scenarios.

### B. Domain Adaptation

Domain adaptation [1], [2] aims to boost performance in the target domain by leveraging essential knowledge from the source domain. Lots of domain adaptation methods dedicate to reducing domain discrepancies by learning domain-invariant feature representations. Methods along this line can be generally categorized into two types: criterion-based methods [6], [28], [43], [44], [57], [69], [84] and adversarial learning-based methods [7], [9], [10], [15], [16], [29], [72], [73], [80], [88], [89]. The former aligns feature distributions between different domains by minimizing some statistics, such as Maximum Mean Discrepancy [44], Correlation Alignment [69], Wasserstein distance [28], and HoMM [6]. The latter introduces a domain discriminator to classify feature representations, while adversarially confuses the discriminator by constructing a minimax game with the feature extractor. These methods have been widely studied and achieved superior performance in image classification [12], [15], [25], [58], semantic segmentation [13], [47], [52], [62], [71], [78], [82], object detection [3], [11], [26], [59], [66], [92], [95].

However, domain adaptation for crowd counting is less studied, and existing generic methods cannot easily adapt to crowd counting due to its special labeling mechanism and diverse backgrounds in crowd scenes.

### C. Domain Adaptation for Crowd Counting

Recently, some methods are proposed to solve domain adaptation for crowd counting. They can be mainly grouped into three categories, including (i) *pixel-level adaptation methods* [18], [76]: [76] constructs a synthetic dataset GCC and modifies CycleGAN [94] to conduct style transfer to generate target-domain crowd images for supervised training. [18] improves the style transfer mechanism in [76] by the separation of domain-shared feature extraction and domain-invariant feature decoration. (ii) *feature-level adaptation methods* [19]–[21]: Gao *et al.* [19] propose to discriminate features across domains and constrain density map generation by source-domain pseudo labels. Han *et al.* [20] constrain the feature extraction by a feature discriminator and an auxiliary semantic task. Hossain *et al.* [21] reduce the domain shift by minimizing the feature distances (i.e., Maximum Mean Discrepancy (MMD) [44]) across domains. (iii) *others* [41], [77]: [41] introduce an extra head detector for mutual training with the crowd counter. [77] present a neuron linear transformation to

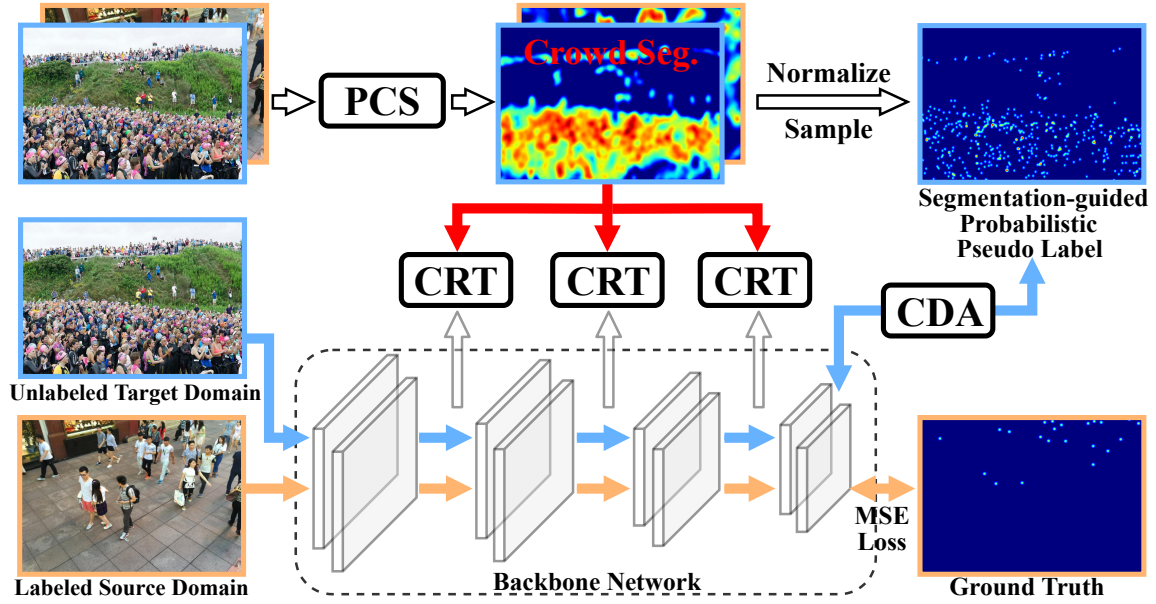


Fig. 2: Overview of the proposed fine-grained domain adaptation framework for crowd counting. Instead of viewing each crowd image as a whole, we propose to learn crowd segmentation from point-level crowd counting annotations, namely Point-derived Crowd Segmentation (PCS) to guide crowd features transfer across domains beyond background distractions in the Crowd Region Transfer (CRT) module. Additionally, we further exploit PCS to generate Segmentation-guided Probabilistic Pseudo Labels (SPPL) to align target-domain crowd density distributions in the Crowd Density Alignment (CDA) module.

optimize a small amount of parameters based on few target-domain training samples. Methods in *others* can be regarded as supplements of pixel-level and feature-level methods with additional bounding box annotations [41] or extra target-domain annotations [77].

Notwithstanding the demonstrated success of the above methods, they all conduct domain adaptation on crowds and backgrounds simultaneously in a holistic manner. However, crowds and backgrounds have different characteristics and backgrounds may vary dramatically in different scenes. Domain transfer between crowds and backgrounds inevitably incurs misalignment, leaving room for improvement of previous methods. Differently, the proposed method proposes to treat crowd and background differently and derive crowd segmentation from crowd counting datasets for fine-grained domain adaptation for crowd counting.

### III. METHOD

#### A. Problem Formulation

In the task of cross-domain crowd counting, we are given a labeled source domain  $\mathcal{D}_S = \{(\mathbf{x}_i^s, \mathbf{y}_i^s)\}_{i=1}^{N_s}$ , where  $\mathbf{x}_i^s$  and  $\mathbf{y}_i^s$  denote the  $i$ -th crowd image and the corresponding label, i.e., the coordinates of head centers indicating head positions. Besides, we have access to a unlabeled target domain  $\mathcal{D}_T = \{(\mathbf{x}_i^t)\}_{i=1}^{N_t}$  containing a set of unlabeled crowd images. We assume that samples from the two domains are drawn from different distributions, and our goal is to improve the counting performance in the unlabeled target domain  $\mathcal{D}_T$  utilizing the knowledge from both domains.

#### B. Framework Overview

As shown in Fig. 2, we propose a Crowd-aware domain Adaptation framework for Crowd Counting (CACC), which contains a crowd counter, a Point-derived Crowd Segmentation (PCS) network, and two adaptation modules, i.e., Crowd Region Transfer (CRT) and Crowd Density Alignment (CDA). **Crowd Counter.** Most crowd counting networks employ density maps as the intermediate output for better supervision. They are typically generated by convolving each annotated head point with a Gaussian kernel [90]:

$$\mathcal{D}(\mathbf{z}) = \sum_{k=1}^N \delta(\mathbf{z} - \mathbf{z}_k) * G_{\sigma_k}(\mathbf{z}), \quad (1)$$

where  $\mathbf{z}$  and  $\mathbf{z}_k$  denote each pixel and the  $k$ -th annotated point (total  $N$  points) in a crowd image  $\mathbf{x}$ .  $G_{\sigma_k}$  is a 2D Gaussian kernel with a bandwidth  $\sigma_k$ . Following previous works [19], [20], [76], we employ a simple and universal crowd counter without specialized techniques to verify the general effectiveness of the proposed domain adaptation method. Specifically, we extract the first ten convolutional layers of VGG16 [64] with three maxpooling layers as the backbone network. After the backbone network, we introduce several deconvolutional layers to generate high-resolution density maps. To measure the distance between the ground truth and the estimated density map, we adopt the widely-used pixel-wise Euclidean loss which can be formulated as:

$$\mathcal{L}_{den}(\mathbf{x}) = \frac{1}{2M} \|\mathbf{D}^{est}(\mathbf{x}) - \mathbf{D}^{GT}(\mathbf{x})\|_2^2 \quad (2)$$

where  $M$  is the number of pixels in the input image  $\mathbf{x}$ .  $\mathbf{D}^{est}(\mathbf{x})$  and  $\mathbf{D}^{GT}(\mathbf{x})$  represent the estimated and ground truth density maps, respectively.

### C. Point-derived Crowd Segmentation

The Point-derived Crowd Segmentation (PCS) module is designed to learn crowd segmentation from the point-level crowd counting annotations. Although crowd counting annotations does not specify crowd segmentation, they contain information on where crowds appear and how crowds look like. We can still extract crowd segmentation by learning the weak label statistics. This is also studied in the context of Multiple Instance Learning (MIL) [49] where a label is assigned to each bag of instances instead of each instance. In our case, we consider each patch cropped from crowd images as a bag of instances (i.e., a set of pixels).

In detail, we densely sample patches from crowd images to construct crowd and background bags  $\mathcal{B} = \{\mathbf{b}_1, \mathbf{b}_2, \dots, \mathbf{b}_N\}$ . The sampling process follows an exhaustive scheme whose core data structure is a set of multi-scale anchors analogous to Faster R-CNN [56]. Each bag  $\mathbf{b}_i$  in  $\mathcal{B}$  contains a set of instances (i.e., pixels)  $\mathbf{X}_i = \{x_1, x_2, \dots, x_{h_i \times w_i}\}$  where  $h_i$  and  $w_i$  are the height and width of  $\mathbf{b}_i$ . Let  $y_j$  be the semantic label of each pixel  $x_j$  in  $\mathbf{X}_i$  which indicates whether it is annotated as a human head position in the crowd counting datasets. Following the standard MIL assumption that negative bags contain only negative instances and positive bags contain at least one positive instance, we automatically partition  $\mathcal{B}$  into crowd bags  $\mathcal{B}_C$  and background bags  $\mathcal{B}_B$ :

$$\begin{aligned} \mathcal{B}_C &= \{\mathbf{b}_i \in \mathcal{B} \text{ if } y_j = 1, \exists x_j \in \mathbf{b}_i\}, \\ \mathcal{B}_B &= \{\mathbf{b}_i \in \mathcal{B} \text{ if } y_j = 0, \forall x_j \in \mathbf{b}_i\}. \end{aligned} \quad (3)$$

It is worth noting that the annotated crowd positions in the crowd counting datasets focus mainly on human head distributions, and a background bag in Eq. (3) may also contain human bodies below the annotated human heads. To alleviate this problem, we refine the background bags with another two constraints after the cursory partition in Eq. (3):

$$\mathcal{B}'_B = \{\mathbf{b}_i \in \mathcal{B}_B \text{ if } U(\mathbf{b}_i) \notin \mathcal{B}_C \text{ or } L(\mathbf{b}_i) \notin \mathcal{B}_C\}, \quad (4)$$

where  $\mathcal{B}'_B$  is the refined background bags set,  $U(\mathbf{b}_i)$  denotes the directly upper bag of  $\mathbf{b}_i$  towards the upper margin of the whole image,  $L(\mathbf{b}_i)$  represents the larger bags centered at the same location as  $\mathbf{b}_i$ . An example of  $U(\mathbf{b}_i)$  and  $L(\mathbf{b}_i)$  can be seen in Fig. 3. Empirically, we set the height and width of  $L(\mathbf{b}_i)$  as twice of those of  $\mathbf{b}_i$ . For clarity, we use  $\mathcal{B}_B$  instead of  $\mathcal{B}'_B$  to denote the final background bags set.

To learn crowd segmentation from the partitioned bags, we build a weak learner  $\mathcal{F}$  containing several convolution blocks. Given each sample  $\mathbf{b}_i$  from  $\mathcal{B}_C$  or  $\mathcal{B}_B$ ,  $\mathcal{F}$  predicts a 2-channel map  $\mathbf{M}(\mathbf{b}_i) = \mathcal{F}(\mathbf{b}_i, \Theta)$  where  $\Theta$  represents the parameters of  $\mathcal{F}$ . Instead of using pixel-level supervision, we learn  $\mathcal{F}$  with bag-level labels by a standard cross entropy loss:

$$\begin{aligned} \mathcal{L}_{\mathcal{F}} &= \sum_{\mathbf{b}_i \in \mathcal{B}_C} -\log(S(A(\mathbf{M}(\mathbf{b}_i)[0]))) \\ &+ \sum_{\mathbf{b}_i \in \mathcal{B}_B} -\log(S(A(\mathbf{M}(\mathbf{b}_i)[1])), \end{aligned} \quad (5)$$

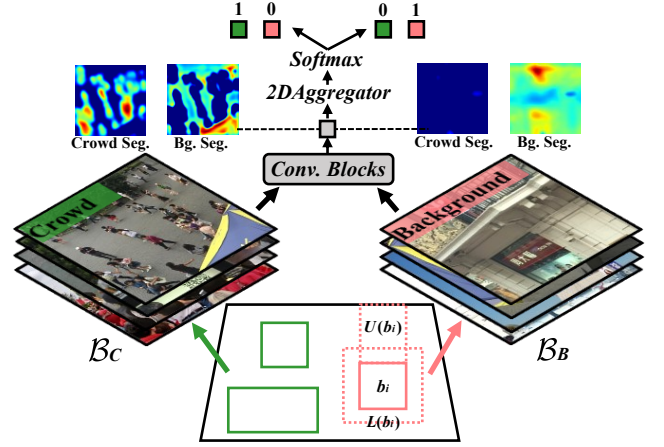


Fig. 3: Learning Point-derived Crowd Segmentation (PCS) from available crowd counting annotations in the context of Multiple Instance Learning [49]. The numbers 0 and 1 in each side constitute a one-hot vector with 1 standing for the label of crowd or background bags.

where  $\mathcal{L}_{\mathcal{F}}$  is the learning objective,  $A(\cdot)$  is a 2D aggregator (e.g., Avg2D),  $S(\cdot)$  denotes the softmax function. The learning of  $\mathcal{F}$  accumulates crowd and background statistics and activates pixel-wise responses  $\mathbf{M}(\mathbf{b}_i)$  for better discrimination of bag labels as shown in Fig. 3. Finally, we use  $\mathbf{M}(\mathbf{b}_i)[0]$  and  $\mathbf{M}(\mathbf{b}_i)[1]$  as crowd and background segmentation respectively for better adaptation across domains.

It is worth noting that with the constraints introduced by the two bags (i.e.,  $U(\mathbf{b}_i)$  and  $L(\mathbf{b}_i)$ ), we may still have some background bags containing human bodies, but the weak learner  $\mathcal{F}$  in Eq. (5) is trained to classify crowd and background bags statistically with natural tolerance to some noisy labels. Experiments in Table I and Fig. 5 demonstrate we can derive high-quality crowd segmentation from point-level annotations for effective fine-grained domain adaptation.

### D. Crowd-aware Domain Adaptation

1) *Crowd Region Transfer*: The Crowd Region Transfer (CRT) module is designed to align crowd features across domains beyond background distractions. It contains two parts: a crowd segmentation mechanism and several domain classifiers.

Given a crowd image  $\mathbf{x}$  from an arbitrary domain, we denote  $\mathbf{C}_{seg} \in \mathbb{R}^{H \times W}$  as the crowd segmentation from the PCS module. As the initial values in  $\mathbf{C}_{seg}$  may be very large or small, we normalize them to the range of [0,1]:

$$\mathbf{C}_{seg}^N = (\mathbf{C}_{seg} - \mathbf{C}_{seg}^{min}) / (\mathbf{C}_{seg}^{max} - \mathbf{C}_{seg}^{min}), \quad (6)$$

where  $\mathbf{C}_{seg}^N$  is the normalized crowd segmentation,  $\mathbf{C}_{seg}^{min}$  and  $\mathbf{C}_{seg}^{max}$  denote the minimum and maximum values in  $\mathbf{C}_{seg}$ , respectively. As  $\mathbf{C}_{seg}^N$  is a soft map with floating-point numbers, we naturally design two variants to disentangle crowds from backgrounds, i.e., soft crowd segmentation  $\mathbf{C}_{seg}^S$  and hard crowd segmentation  $\mathbf{C}_{seg}^H$ . We directly utilize  $\mathbf{C}_{seg}^N$

as  $C_{seg}^S$ . And for  $C_{seg}^H$ , we binarize  $C_{seg}^S$  by comparing it with a given threshold, which can be formulated as:

$$T = \frac{1}{HW} \sum_{h,w} C_{seg}^S(h,w),$$

$$C_{seg}^H = I(C_{seg}^S > T),$$
(7)

where the threshold  $T$  is set to the mean value of  $C_{seg}^S$ , and  $I(\cdot)$  represents the indication function.

To bridge domains in feature representations, we integrate several domain classifiers  $D$  into the feature extraction network  $G$ .  $D$  and  $G$  construct a two-player minimax game, where  $D$  is trained to distinguish which domain the features come from, while  $G$  aims to confuse  $D$ . Existing methods [19], [20] typically regard features from each crowd image as a whole and align features across domains without crowd and background distinction. However, as discussed above, the coarse-grained method inevitably incurs misalignment between crowds and backgrounds, and damages the discriminative features for crowd counting (see Fig. 6 and Sec. IV-E). Therefore, we integrate the derived crowd segmentation with the domain classifiers  $D$ , and design the CRT module for crowd-aware fine-grained feature transfer beyond background distractions. An illustration of the CRT module can be seen in Fig. 4. Specifically, the optimization objective of the CRT module is formulated as:

$$\mathcal{L}_{CRT} = \min_{\theta_G} \max_{\theta_D} \mathbb{E}_{\mathbf{x}_s \sim \mathcal{D}_S} \log D(G(\mathbf{x}_s) \cdot \mathbf{C}_{seg}^{H/S})$$

$$+ \mathbb{E}_{\mathbf{x}_t \sim \mathcal{D}_T} \log(1 - D(G(\mathbf{x}_t) \cdot \mathbf{C}_{seg}^{H/S})),$$
(8)

where  $\theta_G$  and  $\theta_D$  represent the learnable parameters of  $G$  and  $D$ , respectively.  $G(\cdot)$  denotes the extracted domain features which are element-wisely multiplied with hard or soft crowd segmentation  $C_{seg}^{H/S}$  to extract crowd features. As  $G(\cdot)$  extracts multi-scale features, we add a CRT module after each pooling layer (total three pooling layers) in  $G(\cdot)$  in a multi-level fashion. When the training process converges,  $G$  tends to extract domain-invariant crowd feature representations. Combining domain classifiers with the crowd segmentation mechanism, the CRT module realizes crowd features transfer across domains out of the background distractions, which brings out more reliable and customized crowd-aware domain adaptation for crowd counting.

2) *Crowd Density Alignment*: The Crowd Density Alignment (CDA) module is designed to align the target-domain crowd density distributions. As a pioneer work, Gao *et al.* [19] propose to utilize the source-domain density labels to constrain the target-domain density generation. However, different domains usually have different crowd density distributions. It inevitably degrades the adaptation performance to simply apply source-domain density labels. To this end, benefiting from the derived crowd segmentation, we propose to generate Segmentation-guided Probabilistic Pseudo Labels (SPPL) for each target-domain crowd image to directly constrain crowd density generation.

Specifically, we leverage the soft crowd segmentation  $C_{seg}^S \in \mathbb{R}^{H \times W}$  generated by the PCS module as a base,

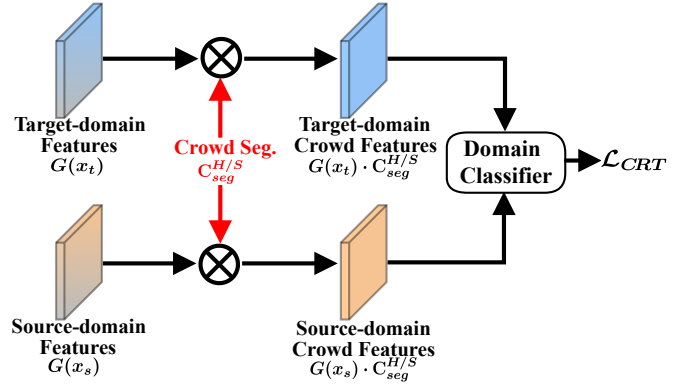


Fig. 4: Illustration of the Crowd Region Transfer (CRT) module. Crowd segmentation  $C_{seg}^{H/S}$  is element-wisely multiplied with domain features to extract crowd features which are discriminated by a domain classifier in  $\mathcal{L}_{CRT}$ .

and generate the probabilistic crowd distribution  $P$  by values normalization as follows:

$$P = C_{seg}^S / \sum_{h,w} C_{seg}^S(h,w),$$
(9)

where  $\sum_{h,w} C_{seg}^S(h,w)$  denotes the sum of all the values in  $C_{seg}^S$ . Therefore, we can formulate  $P$  as a discrete bivariate distribution, and it obeys the following properties:

$$P\{X = w_i, Y = h_j\} = p_{ij},$$

$$p_{ij} \geq 0, \sum_{i=0}^{W-1} \sum_{j=0}^{H-1} p_{ij} = 1,$$

$$0 \leq i \leq W-1, 0 \leq j \leq H-1.$$
(10)

Then we generate a point set  $\mathcal{P} = \{(w_i, h_i) | i \in [1, n]\}$  indicating pseudo crowd positions by iteratively sampling  $n$  coordinates obeying Eq. (10). Note that  $n$  should be consistent with the number of people which is not given in the unlabeled target domain. Therefore, we predict an initial approximate crowd count based on the pre-trained model in the source-domain. With the domain adaptation, we dynamically update  $n$  by the new estimation of the adapted model in an inertial way, which can be formulated as:

$$\alpha = |n^{(k-1)} - est^{(k)}| / \max(n^{(k-1)}, est^{(k)}),$$

$$n^{(k)} = \alpha n^{(k-1)} + (1 - \alpha) est^{(k)},$$
(11)

where  $\alpha$  is the updating coefficient.  $n^{(k)}$  and  $est^{(k)}$  denote the sampling and estimated crowd counts at  $k$ -th iteration.

With the pseudo point set  $\mathcal{P}$  indicating crowd positions, we convolve each point in  $\mathcal{P}$  following Eq. (1) to generate Segmentation-guided Probabilistic Pseudo Labels (SPPL). Then we introduce adversarial training to align target-domain crowd density distributions with SPPL as follows:

$$\mathcal{L}_{CDA} = \min_{\theta_G} \max_{\theta_{D_m}} \mathbb{E}_{\mathbf{M}_{SPPL} \sim \mathcal{D}_{SPPL}} \log D_m(\mathbf{M}_{SPPL})$$

$$+ \mathbb{E}_{\mathbf{x}_t \sim \mathcal{D}_T} \log(1 - D_m(G(\mathbf{x}_t))),$$
(12)

where  $D_m$  denotes the crowd density discriminator different from the crowd feature discriminator  $D$  in Eq. (8),  $\mathbf{M}_{SPPL}$  and

---

**Algorithm 1:** Crowd-aware Domain Adaption for Crowd Counting.

---

**Input:** Labeled source domain  $\mathcal{D}_S$ .

Unlabeled target domain  $\mathcal{D}_T$ . Batch size  $B$ .

**Output:** An adaptive crowd counter  $C(\cdot, \theta)$ .

- 1 Sample bags  $\mathcal{B}$  in  $\mathcal{D}_S$  and partition  $\mathcal{B}$  into  $\mathcal{B}_C$  and  $\mathcal{B}_B$  by Eq. (3) and Eq. (4).
  - 2 Weak learning of  $\mathcal{F}$  on  $\mathcal{B}_C$  and  $\mathcal{B}_B$  by Eq. (5).
  - 3 Obtain crowd segmentation in  $\mathcal{D}_S$  and  $\mathcal{D}_T$ .
  - 4 Supervised learning of  $C(\cdot, \theta)$  in  $\mathcal{D}_S$ .
  - 5 Calculate initial sampling number  $n^{(0)}$  in Eq. (11).
  - 6 **for**  $i = 1$  **to**  $max\_iter$  **do**
  - 7      $X_S, Y_S \leftarrow Sample(\mathcal{D}_S, B/2)$
  - 8      $X_T \leftarrow Sample(\mathcal{D}_T, B/2)$
  - 9     Calculate  $\mathcal{L}_{den}$  by Eq. (2)
  - 10    Calculate  $\mathcal{L}_{CRT}$  by Eq. (8)
  - 11    Generate SPPL by Eq. (9) and Eq. (10)
  - 12    Calculate  $\mathcal{L}_{CDA}$  according to Eq. (12)
  - 13    Optimize  $C(\cdot, \theta)$  by Eq. (13)
  - 14    Update sampling number  $n^{(i)}$  by Eq. (11)
- 

$\mathcal{D}_{SPPL}$  represent the generated SPPL maps and the corresponding domain, respectively. With the SPPL-based crowd density alignment, our method can directly constrain the target-domain density generation with the local Gaussian prior and global crowd distributions simultaneously, which results in superior adaptation performance.

### E. Network Optimization

The training procedure of the proposed framework contains three major components: Supervised Learning (SL)  $\mathcal{L}_{den}$ , Crowd Region Transfer (CRT)  $\mathcal{L}_{CRT}$ , and Crowd Density Alignment (CDA)  $\mathcal{L}_{CDA}$ . With the above terms, the overall optimization objective can be written as:

$$\mathcal{L}_{total} = \mathcal{L}_{den} + \lambda_1 \mathcal{L}_{CRT} + \lambda_2 \mathcal{L}_{CDA}, \quad (13)$$

where  $\lambda_1$  and  $\lambda_2$  are factors to balance the three items. The detailed optimization procedure is shown in Algorithm 1.

## IV. EXPERIMENTS

### A. Datasets and Scenarios

**Datasets.** Four datasets are used in our experiments. (i) **GCC** [76] is a synthetic dataset containing 15,212 images with resolution of  $1080 \times 1920$ , which are rendered by GTA5 and captured by 400 surveillance cameras in a fictional city. (ii) **SHPartA** [90] is randomly crawled from the Internet with various crowd scenes containing 482 images, in which 300 images for training and 182 images for testing. (iii) **SHPartB** [90] is collected from the busy streets of metropolitan areas in Shanghai consisting of 716 images, in which 400 images for training and the remaining for testing. Compared to SHPartA, SHPartB has relatively fixed camera perspectives and crowd scenes. (iv) **JHU-CROWD (JHUC)** [65] is a large-scale dataset proposed recently, which contains 4,372 images. Images are collected under a variety of scenes and environmental conditions, and

annotations include head positions, approximate sizes, blur-level, occlusion-level, weather-labels, *etc.*

**Scenarios.** We evaluate the adaptation performance under three circumstances as follows: (i) **Synthetic-to-Real** (GCC $\rightarrow$ SHPartB, GCC $\rightarrow$ SHPartA). Synthetic datasets offer an alternative way to alleviate the labeling burden. To reduce the gap between the synthetic and real crowd scenes, we employ GCC as the source domain and the training set of SHPartB or SHPartA as the target domain. (ii) **Fixed-to-Fickle** (SHPartB  $\rightarrow$  SHPartA). Images captured in different crowd scenes also incur domain discrepancies. To simulate it, we utilize the training set of SHPartB (a fixed crowd scene) as the source domain and the training set of SHPartA (various crowd scenes) as the target domain. Note that instead of choosing a target domain with one fixed crowd scene, we propose to utilize SHPartA with various crowd scenes, which is a more challenging setting and has more practical values. (iii) **Normal-to-BadWeather** (SHPartA $\rightarrow$ JHUC). Bad weather sometimes appears in camera surveillance. To simulate weather condition changes, we utilize the training set of SHPartA as the source domain and the images with bad weather conditions in the training set of JHUC as the target domain. *Note that the previous cross-domain crowd counting methods only evaluate their performance on Synthetic-to-Real. However, we believe it is not enough as more real-world datasets are annotated in crowd counting, Real-to-Real should raise more attention because of its natural advantages.*

### B. Implementation Details

In all experiments, we set the batch size as 2, i.e., one image per domain. Following previous methods, we adopt random cropping and horizontal flipping for data augmentation. Adam optimizer [27] is utilized to optimize the networks with the learning rate of the crowd counter and all classifiers initialized as  $10^{-4}$  and  $10^{-5}$ , respectively.  $\lambda_1$  and  $\lambda_2$  in Eq. (13) are set to 1 and 0.3 respectively via cross validation. Following [76], Scene Regularization is utilized to select synthetic images from GCC to facilitate adaptation. The training and evaluation are achieved on NVIDIA GTX 2080Ti GPU. Following previous methods, Mean Absolute Error (MAE) and Root Mean Squared Error (RMSE) are utilized as the evaluation metrics, which are formulated as:

$$MAE = \frac{1}{S} \sum_{i=1}^S |\hat{C}_i - C_i^{GT}|, \quad (14)$$

$$RMSE = \sqrt{\frac{1}{S} \sum_{i=1}^S |\hat{C}_i - C_i^{GT}|^2}, \quad (15)$$

where  $S$  is the number of testing samples.  $\hat{C}_i$  and  $C_i^{GT}$  are the estimated and ground-truth crowd counts of the  $i$ -th sample which are calculated by summing over the entire density maps.

### C. Ablation Studies

We conduct extensive ablation studies in the Synthetic-to-Real adaptation scenario to validate the effectiveness of the proposed modules, i.e., PCS, CRT, and CDA.



Fig. 5: Qualitative results of Point-derived Crowd Segmentation (PCS) in the Synthetic-to-Real adaptation scenario. Warmer colors mean higher values.

**Baselines.** “Source only” denotes the crowd counter trained on the source domain only. “CRT w/o PCS” means removing the segmentation mechanism in the CRT module and transferring features across domains in a holistic manner. “CRT&BRT w/ PCS” represents utilizing the crowd and background segments derived from PCS to guide crowd features Transfer (CRT) and background features transfer (BRT), respectively. “CRT w/ PCS” represents the whole CRT module with soft crowd segmentation derived from PCS. “CRT w/ PCS&Hard Seg.” denotes the CRT module with hard crowd segmentation defined in Eq. (7). “SDA [19]” means Source-domain Density Alignment [19] which utilizes source-domain density labels to constrain the target-domain density generation.

**Effectiveness of PCS.** Since crowd segmentation is not labeled in crowd counting datasets, we evaluate PCS by testing whether PCS covers all annotated human heads. The percentages of coverage in the Synthetic-to-Real adaptation scenario are 98.5, 93.6, and 95.2 for GCC, SHPartA, and SHPartB datasets, respectively, which indicates that almost all human heads can be covered by PCS. Some qualitative results of PCS are shown in Fig. 5. As PCS is the base of the proposed CRT and CDA modules, we further verify PCS by evaluating the effectiveness of CRT and CDA in the following parts.

**Effectiveness of CRT.** As shown in Table I, compared to “Source Only”, “CRT w/o PCS” can improve the adaptation performance to some extent. When integrating the PCS module and transferring crowd features and background features across domains separately (namely “CRT&BRT w/ PCS”), additional performance enhancements are found, which demonstrates the effectiveness of the crowd&background disentanglement achieved by the PCS module. After removing “BRT”, “CRT w/ PCS” achieves the highest counting accuracies compared to the other counterparts, which indicates that background features transfer across domains inevitably incurs an adverse effect on the adaptation performance. Besides, “CRT w/ PCS” is better than “CRT w/ PCS&Hard Seg.”. Upon analysis, we find that compared with human bodies, human heads only exist in crowd bags  $\mathcal{B}_C$  in Eq. (3). This enables the activated soft crowd segmentation to focus more on human heads (see Fig. 5) and enhances features transfer around high-density areas, which is crucial for crowd counting due to its head-centric labeling mechanism.

**Effectiveness of CDA.** Based on CRT, we evaluate the effectiveness of CDA in Table II. We can see that “CRT

TABLE I: Ablation studies on the CRT module in the Synthetic-to-Real adaptation scenario.

Method	GCC $\rightarrow$ SHPartB		GCC $\rightarrow$ SHPartA	
	MAE	RMSE	MAE	RMSE
Source only	19.5	28.9	169.2	255.9
CRT w/o PCS	16.4	26.8	134.8	213.6
CRT&BRT w/ PCS	15.8	25.0	128.7	208.3
CRT w/ PCS	<b>14.7</b>	<b>23.5</b>	<b>117.4</b>	<b>201.6</b>
CRT w/ PCS&Hard Seg.	15.0	23.8	122.5	203.2

TABLE II: Ablation studies on the CDA module in the Synthetic-to-Real adaptation scenario. Note that CRT in this table utilizes PCS (also denoted as “CRT w/ PCS” in Table I).

Method	GCC $\rightarrow$ SHPartB		GCC $\rightarrow$ SHPartA	
	MAE	RMSE	MAE	RMSE
CRT	14.7	23.5	117.4	201.6
CRT + SDA [19]	14.3	22.4	114.7	193.7
CRT + CDA	<b>13.5</b>	<b>21.8</b>	<b>109.3</b>	<b>187.1</b>

+ CDA” can outperform “CRT + SDA” consistently, which demonstrates the superiority of the proposed CDA module. Compared to the proposed CDA, SDA [19] uses the source-domain pseudo labels which contain the potential bias from the source-domain crowd distributions, thus limiting the domain adaptation performance.

#### D. Comparison to State-of-the-art Methods

As previous methods do not release their codes and only report their performance in the Synthetic-to-Real adaptation scenario, we compare with them in this scenario and summarize variants of our method in the Fixed-to-Fickle and Normal-to-BadWeather adaptation scenarios. State-of-the-art methods for comparison include: (i) Semi-supervised methods: NLT [77], FSC [20], and (ii) Unsupervised methods: CycleGAN [94], SE CycleGAN [76], Gao et al. [19].

**Synthetic-to-Real.** As shown in Table III, our method can achieve the lowest counting errors and the highest relative gains compared to all the unsupervised counterparts. In particular, we achieve a remarkable gain of 30.7%/24.5% (SHPartB) and 35.4%/26.8% (SHPartA) over the performance before adaptation. Although we do not leverage extra semantic annotations, our method can still outperform FSC [20]. To be comparable with NLT [77], we also introduce 10% labeled target data. The performance of our method in terms of MAE/RMSE is enhanced to 10.2/17.5 (SHPartB) and 82.4/136.6 (SHPartA), respectively, which are better than NLT [77].

**Fixed-to-Fickle & Normal-to-BadWeather.** Results of our method in the two adaptation scenarios are summarized in Table IV and Table V. We can see that the proposed PCS, CRT, and CDA modules can progressively improve the counting accuracies in both scenarios, which confirms the effectiveness of the proposed crowd-aware domain adaptation method in multiple adaptation scenarios.

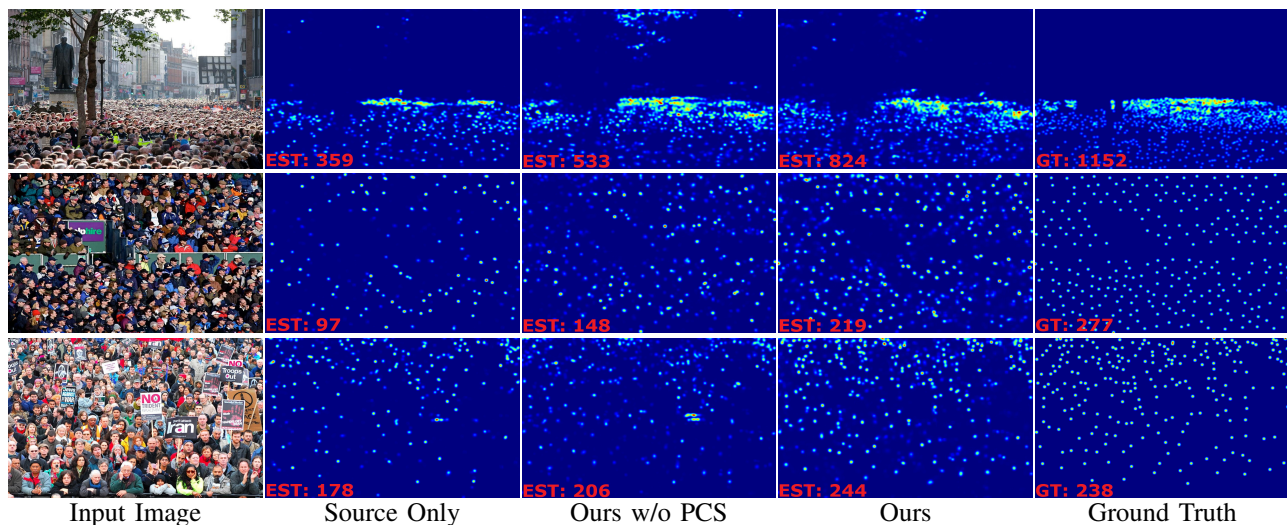


Fig. 6: Qualitative results of the estimated density maps in the Synthetic-to-Real adaptation scenario (best viewed in color). Note that “Ours w/o PCS” also means our method without the CRT and CDA modules as PCS is the base of them.

TABLE III: Comparison with state-of-the-art methods in the Synthetic-to-Real adaptation scenario. “S” and “U” denote the semi-supervised and unsupervised domain adaptation methods, respectively. “Gain” denotes the relative gains of MSE/RMSE in comparison to the performance before adaptation.

		Synthetic → Real					
Method	Type	GCC → SHPartB			GCC → SHPartA		
		MAE ↓	RMSE ↓	Gain ↑	MAE ↓	RMSE ↓	Gains ↑
NLT [77]	S	10.8	18.3	46.2%/37.3%	90.1	151.6	52.0%/45.7%
FSC [20]	S	16.9	24.7	31.1%/26.7%	129.3	187.6	32.2%/37.0%
CycleGAN [94]	U	25.4	39.7	-10.2%/-23.6%	143.3	204.3	10.4%/5.6%
SE CycleGAN [76]	U	19.9	28.3	12.7%/7.5%	123.4	193.4	22.8%/10.6%
Gao <i>et al.</i> [19]	U	16.0	24.7	28.2%/17.3%	–	–	–
Ours (CACC)	U	<b>13.5</b>	<b>21.8</b>	<b>30.7%/24.5%</b>	<b>109.3</b>	<b>187.1</b>	<b>35.4%/26.8%</b>
Oracle	–	8.9	15.3	–	67.5	112.1	–

TABLE IV: Results of the Fixed-to-Fickle adaptation.

Fixed → Fickle (SHPartB → SHPartA)			
Method	MAE ↓	RMSE ↓	Gain ↑
Source only	194.0	298.4	–
CRT w/o PCS	153.2	247.5	21.0%/17.1%
CRT w/ PCS	123.3	204.6	36.4%/31.4%
CRT w/ PCS + CDA (full)	<b>115.6</b>	<b>199.5</b>	<b>40.4%/33.1%</b>
Oracle	67.5	112.1	–

TABLE V: Results of the Normal-to-BadWeather adaptation.

Normal → BadWeather (SHPartA → JHUC)			
Method	MAE ↓	RMSE ↓	Gain ↑
Source only	208.5	535.6	–
CRT w/o PCS	173.6	437.2	16.7%/18.3%
CRT w/ PCS	159.5	394.7	23.5%/26.3%
CRT w/ PCS + CDA (full)	<b>153.2</b>	<b>384.0</b>	<b>26.5%/28.3%</b>
Oracle	80.4	215.3	–

### E. Qualitative Results

Qualitative results of the estimated density maps can be seen in Fig. 6. Due to the domain shift problem, the “Source Only” model simply detects some salient individuals in the crowd. From “Source Only” to “Ours w/o PCS”, we can observe that the “Ours w/o PCS” model can increase true positives to some extent, but also incurs some false positives in the background areas due to the misalignment between crowds and backgrounds. Differently, our method can consistently estimate more accurate crowd densities and suppresses the occurrence of false positives thanks to the proposed crowd-

aware fine-grained domain adaptation method.

### V. CONCLUSION

In this paper, we propose to untangle crowds and backgrounds from crowd images and design a Crowd-aware fine-grained domain Adaptation framework for Crowd Counting (CACC). Specifically, we propose a novel and effective schema to learn crowd segmentation from pixel-level crowd counting annotations without extra labeling efforts in the context of Multiple Instance Learning. Based on the derived segments, we design two novel crowd-aware adaptation modules, namely

Crowd Region Transfer (CRT) and Crowd Density Alignment (CDA). Extensive experiments in multiple cross-domain scenarios demonstrate the superiority of the proposed method.

## REFERENCES

- [1] S. Ben-David, J. Blitzer, K. Crammer, A. Kulesza, F. Pereira, and J. W. Vaughan. A theory of learning from different domains. *Machine learning*, 79(1-2):151–175, 2010. 2
- [2] S. Ben-David, J. Blitzer, K. Crammer, and F. Pereira. Analysis of representations for domain adaptation. In *NeurIPS*, 2007. 2
- [3] Q. Cai, Y. Pan, C.-W. Ngo, X. Tian, L. Duan, and T. Yao. Exploring object relation in mean teacher for cross-domain detection. In *CVPR*, 2019. 2
- [4] X. Cao, Z. Wang, Y. Zhao, and F. Su. Scale aggregation network for accurate and efficient crowd counting. In *ECCV*, 2018. 2
- [5] L. Chai, Y. Liu, W. Liu, G. Han, and S. He. Crowdgan: Identity-free interactive crowd video generation and beyond. *TPAMI*, (01):1–1, 2020. 2
- [6] C. Chen, Z. Fu, Z. Chen, S. Jin, Z. Cheng, X. Jin, and X.-S. Hua. Homm: Higher-order moment matching for unsupervised domain adaptation. In *AAAI*, 2020. 2
- [7] C. Chen, W. Xie, W. Huang, Y. Rong, X. Ding, Y. Huang, T. Xu, and J. Huang. Progressive feature alignment for unsupervised domain adaptation. In *CVPR*, 2019. 2
- [8] K. Chen, C. C. Loy, S. Gong, and T. Xiang. Feature mining for localised crowd counting. In *BMVC*, 2012. 2
- [9] M. Chen, S. Zhao, H. Liu, and D. Cai. Adversarial-learned loss for domain adaptation. In *AAAI*, 2020. 2
- [10] Q. Chen, Y. Liu, Z. Wang, I. Wassell, and K. Chetty. Re-weighted adversarial adaptation network for unsupervised domain adaptation. In *CVPR*, 2018. 2
- [11] Y. Chen, W. Li, C. Sakaridis, D. Dai, and L. Van Gool. Domain adaptive faster r-cnn for object detection in the wild. In *CVPR*, 2018. 2
- [12] Z. Ding, S. Li, M. Shao, and Y. Fu. Graph adaptive knowledge transfer for unsupervised domain adaptation. In *ECCV*, 2018. 2
- [13] L. Du, J. Tan, H. Yang, J. Feng, X. Xue, Q. Zheng, X. Ye, and X. Zhang. Ssf-dan: Separated semantic feature based domain adaptation network for semantic segmentation. In *ICCV*, 2019. 2
- [14] N. Elassal and J. H. Elder. Unsupervised crowd counting. In *ACCV*, 2016. 2
- [15] Y. Ganin and V. Lempitsky. Unsupervised domain adaptation by backpropagation. In *ICML*, 2015. 2
- [16] Y. Ganin, E. Ustinova, H. Ajakan, P. Germain, H. Larochelle, F. Laviolette, M. Marchand, and V. Lempitsky. Domain-adversarial training of neural networks. *The Journal of Machine Learning Research*, 17(1):2096–2030, 2016. 2
- [17] G. Gao, J. Gao, Q. Liu, Q. Wang, and Y. Wang. Cnn-based density estimation and crowd counting: A survey. *arXiv preprint arXiv:2003.12783*, 2020. 1
- [18] J. Gao, T. Han, Q. Wang, and Y. Yuan. Domain-adaptive crowd counting via inter-domain features segregation and gaussian-prior reconstruction. *arXiv preprint arXiv:1912.03677*, 2019. 2
- [19] J. Gao, Q. Wang, et al. Feature-aware adaptation and density alignment for crowd counting in video surveillance. *TCYB*, 2020. 1, 2, 3, 5, 7, 8
- [20] T. Han, J. Gao, Y. Yuan, and Q. Wang. Focus on semantic consistency for cross-domain crowd understanding. In *ICASSP*, 2020. 1, 2, 3, 5, 7, 8
- [21] M. A. Hossain, M. K. K. Reddy, K. Cannons, Z. Xu, and Y. Wang. Domain adaptation in crowd counting. In *CRV*, 2020. 1, 2
- [22] H. Idrees, I. Saleemi, C. Seibert, and M. Shah. Multi-source multi-scale counting in extremely dense crowd images. In *CVPR*, 2013. 2
- [23] X. Jiang, Z. Xiao, B. Zhang, X. Zhen, X. Cao, D. Doermann, and L. Shao. Crowd counting and density estimation by trellis encoder-decoder networks. In *CVPR*, 2019. 2
- [24] X. Jiang, L. Zhang, M. Xu, T. Zhang, P. Lv, B. Zhou, X. Yang, and Y. Pang. Attention scaling for crowd counting. In *CVPR*, 2020. 2
- [25] G. Kang, L. Jiang, Y. Yang, and A. G. Hauptmann. Contrastive adaptation network for unsupervised domain adaptation. In *CVPR*, 2019. 2
- [26] T. Kim, M. Jeong, S. Kim, S. Choi, and C. Kim. Diversify and match: A domain adaptive representation learning paradigm for object detection. In *CVPR*, 2019. 2
- [27] D. P. Kingma and J. Ba. Adam: A method for stochastic optimization. *arXiv preprint arXiv:1412.6980*, 2014. 6
- [28] C.-Y. Lee, T. Batra, M. H. Baig, and D. Ulbricht. Sliced wasserstein discrepancy for unsupervised domain adaptation. In *CVPR*, 2019. 2
- [29] S. Lee, D. Kim, N. Kim, and S.-G. Jeong. Drop to adapt: Learning discriminative features for unsupervised domain adaptation. In *ICCV*, 2019. 2
- [30] V. Lempitsky and A. Zisserman. Learning to count objects in images. In *NeurIPS*, 2010. 2
- [31] T. Li, H. Chang, M. Wang, B. Ni, R. Hong, and S. Yan. Crowded scene analysis: A survey. *TCSVT*, 25(3):367–386, 2014. 1
- [32] Y. Li, X. Zhang, and D. Chen. Csrnet: Dilated convolutional neural networks for understanding the highly congested scenes. In *CVPR*, 2018. 2
- [33] D. Lian, J. Li, J. Zheng, W. Luo, and S. Gao. Density map regression guided detection network for rgb-d crowd counting and localization. In *CVPR*, 2019. 2
- [34] Z. Lin and L. S. Davis. Shape-based human detection and segmentation via hierarchical part-template matching. *TPAMI*, 32(4):604–618, 2010. 2
- [35] L. Liu, H. Lu, H. Zou, H. Xiong, Z. Cao, and C. Shen. Weighing counts: Sequential crowd counting by reinforcement learning. In *ECCV*, 2020. 2
- [36] N. Liu, Y. Long, C. Zou, Q. Niu, L. Pan, and H. Wu. Adcrowdnet: An attention-injective deformable convolutional network for crowd understanding. In *CVPR*, 2019. 2
- [37] W. Liu, M. Salzmann, and P. Fua. Context-aware crowd counting. In *CVPR*, 2019. 2
- [38] X. Liu, J. Van De Weijer, and A. D. Bagdanov. Leveraging unlabeled data for crowd counting by learning to rank. In *CVPR*, 2018. 2
- [39] X. Liu, J. Van De Weijer, and A. D. Bagdanov. Exploiting unlabeled data in cnns by self-supervised learning to rank. *TPAMI*, 41(8):1862–1878, 2019. 2
- [40] Y. Liu, L. Liu, P. Wang, P. Zhang, and Y. Lei. Semi-supervised crowd counting via self-training on surrogate tasks. In *ECCV*, 2020. 2
- [41] Y. Liu, Z. Wang, M. Shi, S. Satoh, Q. Zhao, and H. Yang. Towards unsupervised crowd counting via regression-detection bi-knowledge transfer. In *ACM Int. Conf. Multimedia*, 2020. 2, 3
- [42] Y. Liu, Q. Wen, H. Chen, W. Liu, J. Qin, G. Han, and S. He. Crowd counting via cross-stage refinement networks. *TIP*, 29:6800–6812, 2020. 2
- [43] M. Long, Y. Cao, Z. Cao, J. Wang, and M. I. Jordan. Transferable representation learning with deep adaptation networks. *TPAMI*, 41(12):3071–3085, 2018. 2
- [44] M. Long, H. Zhu, J. Wang, and M. I. Jordan. Deep transfer learning with joint adaptation networks. In *ICML*, 2017. 2
- [45] C. C. Loy, K. Chen, S. Gong, and T. Xiang. Crowd counting and profiling: Methodology and evaluation. In *Modeling, simulation and visual analysis of crowds*, pages 347–382, 2013. 1
- [46] A. Luo, F. Yang, X. Li, D. Nie, Z. Jiao, S. Zhou, and H. Cheng. Hybrid graph neural networks for crowd counting. In *AAAI*, 2020. 2
- [47] Y. Luo, L. Zheng, T. Guan, J. Yu, and Y. Yang. Taking a closer look at domain shift: Category-level adversaries for semantics consistent domain adaptation. In *CVPR*, 2019. 2
- [48] Z. Ma, X. Wei, X. Hong, and Y. Gong. Bayesian loss for crowd count estimation with point supervision. In *ICCV*, 2019. 2
- [49] O. Maron and T. Lozano-Pérez. A framework for multiple-instance learning. *NeurIPS*, pages 570–576, 1998. 2, 4
- [50] Y. Miao, Z. Lin, G. Ding, and J. Han. Shallow feature based dense attention network for crowd counting. In *AAAI*, 2020. 2
- [51] M.-h. Oh, P. A. Olsen, and K. N. Ramamurthy. Crowd counting with decomposed uncertainty. In *AAAI*, 2020. 2
- [52] F. Pan, I. Shin, F. Rameau, S. Lee, and I. S. Kweon. Unsupervised intra-domain adaptation for semantic segmentation through self-supervision. In *CVPR*, 2020. 2
- [53] S. J. Pan and Q. Yang. A survey on transfer learning. *TKDE*, 22(10):1345–1359, 2009. 1
- [54] V. Ranjan, B. Wang, M. Shah, and M. Hoai. Uncertainty estimation and sample selection for crowd counting. In *ACCV*, 2020. 2
- [55] M. K. K. Reddy, M. Hossain, M. Rochan, and Y. Wang. Few-shot scene adaptive crowd counting using meta-learning. In *WACV*, 2020. 2
- [56] S. Ren, K. He, R. Girshick, and J. Sun. Faster r-cnn: Towards real-time object detection with region proposal networks. *TPAMI*, 39(6):1137, 2017. 4
- [57] A. Rozantsev, M. Salzmann, and P. Fua. Residual parameter transfer for deep domain adaptation. In *CVPR*, 2018. 2
- [58] K. Saito, Y. Ushiku, and T. Harada. Asymmetric tri-training for unsupervised domain adaptation. In *ICML*, 2017. 2
- [59] K. Saito, Y. Ushiku, T. Harada, and K. Saenko. Strong-weak distribution alignment for adaptive object detection. In *CVPR*, 2019. 2
- [60] D. B. Sam, N. N. Sajjan, H. Maurya, and R. V. Babu. Almost unsupervised learning for dense crowd counting. In *AAAI*, 2019. 2
- [61] D. B. Sam, S. Surya, and R. V. Babu. Switching convolutional neural network for crowd counting. In *CVPR*, 2017. 2

- [62] S. Sankaranarayanan, Y. Balaji, A. Jain, S. Nam Lim, and R. Chellappa. Learning from synthetic data: Addressing domain shift for semantic segmentation. In *CVPR*, 2018. [2](#)
- [63] M. Shi, Z. Yang, C. Xu, and Q. Chen. Revisiting perspective information for efficient crowd counting. In *CVPR*, 2019. [2](#)
- [64] K. Simonyan and A. Zisserman. Very deep convolutional networks for large-scale image recognition. *arXiv preprint arXiv:1409.1556*, 2014. [3](#)
- [65] V. Sindagi, R. Yasarla, and V. M. Patel. Jhu-crowd++: Large-scale crowd counting dataset and a benchmark method. *TPAMI*, 2020. [1](#), [6](#)
- [66] V. A. Sindagi, P. Oza, R. Yasarla, and V. M. Patel. Prior-based domain adaptive object detection for hazy and rainy conditions. In *ECCV*, 2020. [2](#)
- [67] V. A. Sindagi and V. M. Patel. Ha-ccn: Hierarchical attention-based crowd counting network. *TIP*, 29:323–335, 2019. [2](#)
- [68] V. A. Sindagi, R. Yasarla, D. S. Babu, R. V. Babu, and V. M. Patel. Learning to count in the crowd from limited labeled data. *arXiv preprint arXiv:2007.03195*, 2020. [2](#)
- [69] B. Sun and K. Saenko. Deep coral: Correlation alignment for deep domain adaptation. In *ECCV*, 2016. [2](#)
- [70] A. Torralba and A. A. Efros. Unbiased look at dataset bias. In *CVPR*, 2011. [1](#)
- [71] Y.-H. Tsai, W.-C. Hung, S. Schulter, K. Sohn, M.-H. Yang, and M. Chandraker. Learning to adapt structured output space for semantic segmentation. In *CVPR*, 2018. [2](#)
- [72] E. Tzeng, J. Hoffman, K. Saenko, and T. Darrell. Adversarial discriminative domain adaptation. In *CVPR*, 2017. [2](#)
- [73] R. Volpi, P. Morerio, S. Savarese, and V. Murino. Adversarial feature augmentation for unsupervised domain adaptation. In *CVPR*, 2018. [2](#)
- [74] J. Wan and A. Chan. Adaptive density map generation for crowd counting. In *ICCV*, 2019. [2](#)
- [75] M. Wang and X. Wang. Automatic adaptation of a generic pedestrian detector to a specific traffic scene. In *CVPR*, 2011. [2](#)
- [76] Q. Wang, J. Gao, W. Lin, and Y. Yuan. Learning from synthetic data for crowd counting in the wild. In *CVPR*, 2019. [1](#), [2](#), [3](#), [6](#), [7](#), [8](#)
- [77] Q. Wang, T. Han, J. Gao, and Y. Yuan. Neuron linear transformation: modeling the domain shift for crowd counting. *TNNLS*, 2021. [2](#), [3](#), [7](#), [8](#)
- [78] Z. Wang, M. Yu, Y. Wei, R. Feris, J. Xiong, W.-m. Hwu, T. S. Huang, and H. Shi. Differential treatment for stuff and things: A simple unsupervised domain adaptation method for semantic segmentation. In *CVPR*, 2020. [2](#)
- [79] B. Wu and R. Nevatia. Detection and tracking of multiple, partially occluded humans by bayesian combination of edgelet based part detectors. *IJCV*, 75(2):247–266, 2007. [2](#)
- [80] M. Xu, J. Zhang, B. Ni, T. Li, C. Wang, Q. Tian, and W. Zhang. Adversarial domain adaptation with domain mixup. In *AAAI*, 2020. [2](#)
- [81] Z. Yan, Y. Yuan, W. Zuo, X. Tan, Y. Wang, S. Wen, and E. Ding. Perspective-guided convolution networks for crowd counting. In *ICCV*, 2019. [2](#)
- [82] J. Yang, R. Xu, R. Li, X. Qi, X. Shen, G. Li, and L. Lin. An adversarial perturbation oriented domain adaptation approach for semantic segmentation. In *AAAI*, 2020. [2](#)
- [83] Y. Yang, G. Li, Z. Wu, L. Su, Q. Huang, and N. Sebe. Weakly-supervised crowd counting learns from sorting rather than locations. In *ECCV*, 2020. [2](#)
- [84] W. Zellinger, T. Grubinger, E. Lughofer, T. Natschläger, and S. Saminger-Platz. Central moment discrepancy (cmd) for domain-invariant representation learning. *arXiv preprint arXiv:1702.08811*, 2017. [2](#)
- [85] A. Zhang, J. Shen, Z. Xiao, F. Zhu, X. Zhen, X. Cao, and L. Shao. Relational attention network for crowd counting. In *ICCV*, 2019. [2](#)
- [86] A. Zhang, L. Yue, J. Shen, F. Zhu, X. Zhen, X. Cao, and L. Shao. Attentional neural fields for crowd counting. In *ICCV*, 2019. [2](#)
- [87] C. Zhang, H. Li, X. Wang, and X. Yang. Cross-scene crowd counting via deep convolutional neural networks. In *CVPR*, 2015. [1](#)
- [88] W. Zhang, W. Ouyang, W. Li, and D. Xu. Collaborative and adversarial network for unsupervised domain adaptation. In *CVPR*, 2018. [2](#)
- [89] Y. Zhang, H. Tang, K. Jia, and M. Tan. Domain-symmetric networks for adversarial domain adaptation. In *CVPR*, 2019. [2](#)
- [90] Y. Zhang, D. Zhou, S. Chen, S. Gao, and Y. Ma. Single-image crowd counting via multi-column convolutional neural network. In *CVPR*, 2016. [1](#), [2](#), [3](#), [6](#)
- [91] Z. Zhao, M. Shi, X. Zhao, and L. Li. Active crowd counting with limited supervision. In *ECCV*, 2020. [2](#)
- [92] Y. Zheng, D. Huang, S. Liu, and Y. Wang. Cross-domain object detection through coarse-to-fine feature adaptation. In *CVPR*, 2020. [2](#)
- [93] Q. Zhou, J. Zhang, L. Che, H. Shan, and J. Z. Wang. Crowd counting with limited labeling through submodular frame selection. *TITS*, 20(5):1728–1738, 2018. [2](#)
- [94] J.-Y. Zhu, T. Park, P. Isola, and A. A. Efros. Unpaired image-to-image translation using cycle-consistent adversarial networks. In *ICCV*, 2017. [1](#), [2](#), [7](#), [8](#)
- [95] X. Zhu, J. Pang, C. Yang, J. Shi, and D. Lin. Adapting object detectors via selective cross-domain alignment. In *CVPR*, 2019. [2](#)